

Adaptive Minimum Symbol Error Rate Beamforming Assisted Detection for Quadrature Amplitude Modulation

S. Chen, A. Livingstone, H.-Q. Du, and L. Hanzo

Abstract—We consider beamforming assisted detection for multiple antenna aided multiuser systems that employ the bandwidth efficient quadrature amplitude modulation scheme. A minimum symbol error rate (MSER) design is proposed for the beamforming assisted receiver, and it is shown that this MSER design provides significant performance enhancement, in terms of achievable symbol error rate, over the standard minimum mean square error (MMSE) design. A sample-by-sample adaptive algorithm, referred to as the least symbol error rate, is derived for adaptive implementation of the MSER beamforming solution. The proposed adaptive MSER scheme is evaluated in simulation using Rayleigh fading channels, in comparison with the adaptive MMSE benchmarker.

Index Terms—Adaptive beamforming, quadrature amplitude modulation, minimum symbol error rate, minimum mean square error.

I. INTRODUCTION

THE ever-increasing demand for mobile communication capacity has motivated the development of antenna array assisted spatial processing techniques [1]–[10] in order to further improve the achievable spectral efficiency. A particular technique that has shown real promise in achieving substantial capacity enhancements is the use of adaptive beamforming with antenna arrays. Adaptive beamforming is capable of separating signals transmitted on the same carrier frequency, and thus provides a practical means of supporting multiusers in a space division multiple access scenario. Classically, the beamforming process is carried out by minimising the mean square error (MSE) between the desired output and the actual array output, and adaptive implementation of this minimum MSE (MMSE) design can be achieved using the well-known least mean square (LMS) algorithm [11],[12]. For a communication system, however, it is the bit error rate (BER) or symbol error rate (SER) that really matters. Recently, adaptive beamforming based on directly minimising the system's BER has been proposed for binary phase shift keying (BPSK) modulation [13]–[18] and quadrature phase shift keying (QPSK) modulation [19],[20]. For the sake of improving the achievable bandwidth efficiency, high-throughput quadrature amplitude modulation (QAM) schemes [21] have

become popular in numerous wireless network standards. The novelty of this work is that we propose the adaptive minimum SER (MSER) beamforming detection scheme for the multiple antenna assisted multiuser system with QAM signalling.

MSER equalisation has been investigated for the single-antenna single-user system with the pulse-amplitude modulation (PAM) scheme [22] and with the QAM scheme [23]. Our proposed adaptive MSER design is very different from the method proposed in [23]. Firstly, the work of [23] did not explicitly derive the SER expression as the function of the equaliser's weight vector. Secondly, and more critically, the adaptive scheme proposed in [23] was not very efficient because adaptation does not take place at the boundary points of the symbol constellation. For the 16-QAM scheme, for example, it means that adaptation does not take place for half of the symbol constellation points and thus half of the training sequence will be wasted. Our adaptive MSER algorithm, referred to as the least symbol error rate (LSER) here, does not suffer from this problem and the scheme has its root in stochastic adaptive approximation of the Parzen window density estimation [24]–[26]. In this sense, our proposed adaptive MSER technique is an extension of the previous method for the PAM equalisation [22] to the interference-limited multiuser communication system employing the QAM scheme. However, the extension from the PAM modulation to the QAM modulation is nontrivial, as will be clearly shown in this work. We also concentrate on investigating the achievable SER performance of the proposed adaptive LSER scheme in Rayleigh fading channels.

The system considered in this study employs L receive antennas to support S users, each having a single transmit antenna. The classic MMSE beamforming design using an antenna array of L elements can create a maximum for the desired user and place $L - 1$ nulls in the directions of the interfering users, provided that they are sufficiently separable in the angular domain. Thus, the system can support up to $S = L$ users. If the number of users S is larger than the number of array elements L , the system is referred to as being rank-deficient, since the system's transfer matrix becomes non-invertible. By contrast, the MSER beamforming design is not restricted by this definition of rank deficiency, which is linked to the minimisation of the mean square error. Thus, the MSER design offers a larger system user capacity than the traditional MMSE design. We will show that the MSER beamforming is more intelligent and it outperforms the MMSE beamforming significantly, particularly in the rank-deficient scenario.

II. SYSTEM MODEL

The system supports S users, and each user employs a single transmit antenna to transmit an M -QAM signal on the

Manuscript received October 17, 2006; revised May 10, 2007; accepted June 18, 2007. The associate editor coordinating the review of this paper and approving it for publication was V. Bhargava. The financial support of the EU under the auspices of the Newcom project is gratefully acknowledged.

S. Chen and L. Hanzo are with the School of Electronics and Computer Science, University of Southampton, Southampton SO17 1BJ, UK (e-mail: sqc@ecs.soton.ac.uk).

A. Livingstone is with Detica, Surrey Research Park, Guildford GU2 7YP, UK.

H.-Q. Du is with the School of Engineering and Electronics, University of Edinburgh, UK.

Digital Object Identifier 10.1109/TWC.2007.060840.

same carrier frequency of $\omega = 2\pi f$. For such a system, user separation can be achieved in the spatial or angular domain [8],[10] and the receiver is equipped with a linear antenna array consisting of L uniformly spaced elements. Assume that the channel is narrow-band which does not induce intersymbol interference. Then the symbol-rate received signal samples can be expressed as

$$x_l(k) = \sum_{i=1}^S A_i b_i(k) e^{j\omega t_l(\theta_i)} + n_l(k) = \bar{x}_l(k) + n_l(k), \quad (1)$$

for $1 \leq l \leq L$, where $t_l(\theta_i)$ is the relative time delay at array element l for source i with θ_i being the direction of arrival for source i , $n_l(k)$ is a complex-valued Gaussian white noise with $E[|n_l(k)|^2] = 2\sigma_n^2$, A_i is the narrow-band channel coefficient for user i , and $b_i(k)$ is the k th symbol of user i which takes the value from the M -QAM symbol set

$$\mathcal{B} \triangleq \{b_{l,q} = u_l + j u_q, 1 \leq l, q \leq \sqrt{M}\} \quad (2)$$

with the real-part symbol $\Re[b_{l,q}] = u_l = 2l - \sqrt{M} - 1$ and the imaginary-part symbol $\Im[b_{l,q}] = u_q = 2q - \sqrt{M} - 1$. Assume that source 1 is the desired-user and the rest of the sources are interfering users. The desired-user signal to noise ratio (SNR) is given by $\text{SNR} = |A_1|^2 \sigma_b^2 / 2\sigma_n^2$ and the desired signal to interferer i ratio (SIR) is $\text{SIR}_i = A_1^2 / A_i^2$, for $2 \leq i \leq S$, where σ_b^2 denotes the M -QAM symbol energy. The received signal vector $\mathbf{x}(k) = [x_1(k) \ x_2(k) \ \dots \ x_L(k)]^T$ can be expressed as

$$\mathbf{x}(k) = \mathbf{P}\mathbf{b}(k) + \mathbf{n}(k) = \bar{\mathbf{x}}(k) + \mathbf{n}(k), \quad (3)$$

where $\mathbf{n}(k) = [n_1(k) \ n_2(k) \ \dots \ n_L(k)]^T$, the system matrix $\mathbf{P} = [A_1 \mathbf{s}_1 \ A_2 \mathbf{s}_2 \ \dots \ A_S \mathbf{s}_S]$ with the steering vector for source i given by $\mathbf{s}_i = [e^{j\omega t_1(\theta_i)} \ e^{j\omega t_2(\theta_i)} \ \dots \ e^{j\omega t_L(\theta_i)}]^T$, and the transmitted QAM symbol vector $\mathbf{b}(k) = [b_1(k) \ b_2(k) \ \dots \ b_S(k)]^T$.

A beamformer is employed, whose soft output is given by

$$y(k) = \mathbf{w}^H \mathbf{x}(k) = \mathbf{w}^H (\bar{\mathbf{x}}(k) + \mathbf{n}(k)) = \bar{y}(k) + e(k) \quad (4)$$

where $\mathbf{w} = [w_1 \ w_2 \ \dots \ w_L]^T$ is the beamformer weight vector and $e(k)$ is Gaussian distributed with zero mean and $E[|e(k)|^2] = 2\sigma_n^2 \mathbf{w}^H \mathbf{w}$. Define the combined system impulse response as $\mathbf{w}^H \mathbf{P} = \mathbf{w}^H [\mathbf{p}_1 \ \mathbf{p}_2 \ \dots \ \mathbf{p}_S] = [c_1 \ c_2 \ \dots \ c_S]$. The beamformer's output can alternatively be expressed as

$$y(k) = c_1 b_1(k) + \sum_{i=2}^S c_i b_i(k) + e(k) \quad (5)$$

where the first term in the righthand side of equation is the desired user signal and the second term is the residual multiuser interference. Note that, in any detection scheme, the main tap c_1 must be known, that is the desired user's channel and associated steering vector, namely $\mathbf{p}_1 = A_1 \mathbf{s}_1$, must be known at the receiver. If this fact is overlooked, the decision will be biased [27]. Provided that $c_1 = c_{R_1} + j c_{I_1}$ satisfies $c_{R_1} > 0$ and $c_{I_1} = 0$, the symbol decision $\hat{b}_1(k) = \hat{b}_{R_1}(k) + j \hat{b}_{I_1}(k)$ can be made as

$$\hat{b}_{R_1}(k) = \begin{cases} u_1, & \text{if } y_R(k) \leq c_{R_1}(u_1 + 1) \\ u_l, & \text{if } c_{R_1}(u_l - 1) < y_R(k) \leq c_{R_1}(u_l + 1) \\ & \text{for } 2 \leq l \leq \sqrt{M} - 1 \\ u_{\sqrt{M}}, & \text{if } y_R(k) > c_{R_1}(u_{\sqrt{M}} - 1) \end{cases} \quad (6)$$

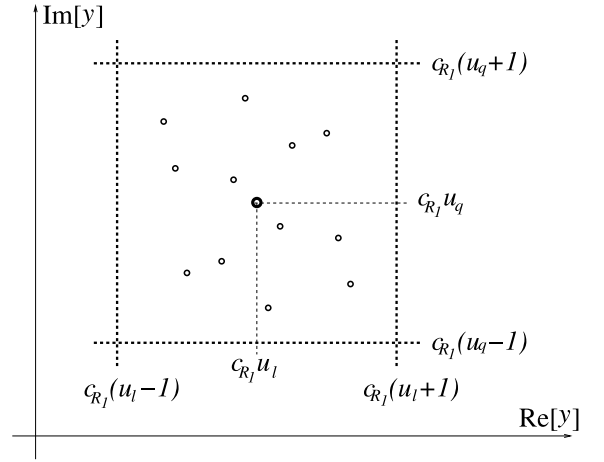


Fig. 1. Decision thresholds associated with point $c_1 b_{l,q}$ assuming $c_{R_1} > 0$ and $c_{I_1} = 0$, and illustrations of symmetric distribution of $\mathcal{Y}_{l,q}$ around $c_1 b_{l,q}$.

$$\hat{b}_{I_1}(k) = \begin{cases} u_1, & \text{if } y_I(k) \leq c_{R_1}(u_1 + 1) \\ u_q, & \text{if } c_{R_1}(u_q - 1) < y_I(k) \leq c_{R_1}(u_q + 1) \\ & \text{for } 2 \leq q \leq \sqrt{M} - 1 \\ u_{\sqrt{M}}, & \text{if } y_I(k) > c_{R_1}(u_{\sqrt{M}} - 1) \end{cases} \quad (7)$$

where $y(k) = y_R(k) + j y_I(k)$ and $\hat{b}_1(k)$ is the estimate for $b_1(k) = b_{R_1}(k) + j b_{I_1}(k)$. Fig. 1 depicts the decision thresholds associated with the decision $\hat{b}_1(k) = b_{l,q}$. In general, $c_1 = \mathbf{w}^H \mathbf{p}_1$ is complex-valued and the rotating operation

$$\mathbf{w}^{\text{new}} = \frac{c_1^{\text{old}}}{|c_1^{\text{old}}|} \mathbf{w}^{\text{old}} \quad (8)$$

can be used to make c_1 real and positive. This rotation is a linear operation and it does not change the system's SER.

III. MINIMUM SYMBOL ERROR RATE BEAMFORMING

The traditional design for the beamformer (4) is the MMSE solution, which can be implemented adaptively using the classical LMS algorithm [11],[12]. The MMSE beamforming design is computationally attractive, because it admits the closed-form solution given the second order statistics of the underlying system. However, since the SER is the true performance indicator, it is desired to consider the optimal MSER Beamforming solution. Denote the $N_b = M^S$ number of legitimate sequences of $\mathbf{b}(k)$ as \mathbf{b}_i , $1 \leq i \leq N_b$. The noise-free part of the received signal $\bar{\mathbf{x}}(k)$ only takes values from the finite signal set defined by $\mathcal{X} \triangleq \{\bar{\mathbf{x}}_i = \mathbf{P}\mathbf{b}_i, 1 \leq i \leq N_b\}$. The set \mathcal{X} can be partitioned into M subsets, depending on the value of $b_1(k)$ as $\mathcal{X}_{l,q} \triangleq \{\bar{\mathbf{x}}_i \in \mathcal{X} : b_1(k) = b_{l,q}\}$, $1 \leq l, q \leq \sqrt{M}$. Similarly the noise-free part of the beamformer's output $\bar{y}(k)$ only takes values from the scalar set $\mathcal{Y} \triangleq \{\bar{y}_i = \mathbf{w}^H \bar{\mathbf{x}}_i, 1 \leq i \leq N_b\}$, and \mathcal{Y} can be divided into the M subsets conditioned on $b_1(k)$

$$\mathcal{Y}_{l,q} \triangleq \{\bar{y}_i \in \mathcal{Y} : b_1(k) = b_{l,q}\}, 1 \leq l, q \leq \sqrt{M}. \quad (9)$$

The following two lemmas summarise the essential properties of the signal subsets $\mathcal{Y}_{l,q}$, $1 \leq l, q \leq \sqrt{M}$, which are useful in the derivation of the SER expression for the beamformer (4).

Lemma 1: The subsets $\mathcal{Y}_{l,q}$, $1 \leq l, q \leq \sqrt{M}$, satisfy the shifting properties

$$\mathcal{Y}_{l+1,q} = \mathcal{Y}_{l,q} + 2c_1, \quad 1 \leq l \leq \sqrt{M} - 1, \quad (10)$$

$$\mathcal{Y}_{l,q+1} = \mathcal{Y}_{l,q} + j2c_1, \quad 1 \leq q \leq \sqrt{M} - 1, \quad (11)$$

$$\mathcal{Y}_{l+1,q+1} = \mathcal{Y}_{l,q} + (2 + j2)c_1, \quad 1 \leq l, q \leq \sqrt{M} - 1. \quad (12)$$

Proof: Any point $\bar{y}_i^{(l+1,q)} \in \mathcal{Y}_{l+1,q}$ can be expressed as

$$\begin{aligned} \bar{y}_i^{(l+1,q)} &= \mathbf{w}^H \mathbf{P} \mathbf{b}_i^{(l+1,q)} = \mathbf{w}^H \mathbf{P} \left(\mathbf{b}_i^{(l,q)} + [2 \ 0 \ \dots \ 0]^T \right) \\ &= \bar{y}_i^{(l,q)} + 2c_1 \end{aligned}$$

where $\bar{y}_i^{(l,q)} \in \mathcal{Y}_{l,q}$. This proves the shifting property (10). Proofs for the other two equations are similar.

Lemma 2: The points of $\mathcal{Y}_{l,q}$ are distributed symmetrically around the symbol point $c_1 b_{l,q}$. This symmetric distribution is with respect to the two horizontal decision boundaries and the two vertical decision boundaries that separate $\mathcal{Y}_{l,q}$ from the other subsets.

Lemma 2 is a direct consequence of symmetric distribution of the symbol constellation (2). This symmetric property is also illustrated in Fig. 1.

For the beamformer with weight vector \mathbf{w} , denote

$$P_E(\mathbf{w}) = \text{Prob}\{\hat{b}_1(k) \neq b_1(k)\}, \quad (13)$$

$$P_{E_R}(\mathbf{w}) = \text{Prob}\{\hat{b}_{R_1}(k) \neq b_{R_1}(k)\}, \quad (14)$$

$$P_{E_I}(\mathbf{w}) = \text{Prob}\{\hat{b}_{I_1}(k) \neq b_{I_1}(k)\}. \quad (15)$$

$P_E(\mathbf{w})$ is the total SER, while $P_{E_R}(\mathbf{w})$ and $P_{E_I}(\mathbf{w})$ are the real-part and imaginary-part SERs, respectively. It is then easy to see that the SER is given by

$$P_E(\mathbf{w}) = P_{E_R}(\mathbf{w}) + P_{E_I}(\mathbf{w}) - P_{E_R}(\mathbf{w})P_{E_I}(\mathbf{w}). \quad (16)$$

From the beamforming model (4) and the signal model (3), the conditional probability density function (PDF) of $y(k)$ given $b_1(k) = b_{l,q}$ is a Gaussian mixture (hence a non-Gaussian PDF) defined by

$$p(y|b_{l,q}) = \frac{1}{N_{sb} 2\pi \sigma_n^2 \mathbf{w}^H \mathbf{w}} \sum_{i=1}^{N_{sb}} e^{-\frac{|y - \bar{y}_i^{(l,q)}|^2}{2\sigma_n^2 \mathbf{w}^H \mathbf{w}}}, \quad (17)$$

where $N_{sb} = N_b/M$ is the size of $\mathcal{Y}_{l,q}$, $\bar{y}_i^{(l,q)} = \bar{y}_{R_i}^{(l,q)} + j\bar{y}_{I_i}^{(l,q)} \in \mathcal{Y}_{l,q}$, and $y = y_R + jy_I$. Noting that c_1 is real-valued and positive and taking into account the symmetric distribution of $\mathcal{Y}_{l,q}$ (lemma 2), for $2 \leq l \leq \sqrt{M} - 1$, the conditional error probability of $\hat{b}_{R_1}(k) \neq u_l$ given $b_{R_1}(k) = u_l$ can be shown to be

$$P_{E_{R,l}}(\mathbf{w}) = \frac{2}{N_{sb}} \sum_{i=1}^{N_{sb}} Q(g_{R_i}^{(l,q)}(\mathbf{w})), \quad (18)$$

where

$$Q(u) = \frac{1}{\sqrt{2\pi}} \int_u^\infty e^{-\frac{z^2}{2}} dz, \quad (19)$$

and

$$g_{R_i}^{(l,q)}(\mathbf{w}) = \frac{\bar{y}_{R_i}^{(l,q)} - c_{R_1}(u_l - 1)}{\sigma_n \sqrt{\mathbf{w}^H \mathbf{w}}}. \quad (20)$$

Further taking into account the shifting property (lemma 1), it can be shown that

$$P_{E_R}(\mathbf{w}) = \gamma \frac{1}{N_{sb}} \sum_{i=1}^{N_{sb}} Q(g_{R_i}^{(l,q)}(\mathbf{w})), \quad (21)$$

where $\gamma = \frac{2\sqrt{M}-2}{\sqrt{M}}$. It is seen that P_{E_R} can be evaluated using (real part of) any single subset $\mathcal{Y}_{l,q}$. Similarly, P_{E_I} can be evaluated using (imaginary part of) any single subset $\mathcal{Y}_{l,q}$ as

$$P_{E_I}(\mathbf{w}) = \gamma \frac{1}{N_{sb}} \sum_{i=1}^{N_{sb}} Q(g_{I_i}^{(l,q)}(\mathbf{w})) \quad (22)$$

with

$$g_{I_i}^{(l,q)}(\mathbf{w}) = \frac{\bar{y}_{I_i}^{(l,q)} - c_{R_1}(u_q - 1)}{\sigma_n \sqrt{\mathbf{w}^H \mathbf{w}}}. \quad (23)$$

Note that the SER is invariant to a positive scaling of \mathbf{w} .

The MSER solution \mathbf{w}_{MSER} is defined as the weight vector that minimises the upper bound of the SER given by

$$P_{E_B}(\mathbf{w}) = P_{E_R}(\mathbf{w}) + P_{E_I}(\mathbf{w}), \quad (24)$$

that is,

$$\mathbf{w}_{\text{MSER}} = \arg \min_{\mathbf{w}} P_{E_B}(\mathbf{w}). \quad (25)$$

The solution obtained by minimising the upper bound (24) is practically equivalent to that of minimising $P_E(\mathbf{w})$, since the bound $P_E(\mathbf{w}) < P_{E_B}(\mathbf{w})$ is very tight, that is, $P_{E_B}(\mathbf{w})$ is very close to the true SER $P_E(\mathbf{w})$. Unlike the MMSE solution, the MSER solution does not admit a closed-form solution. However, the gradients of $P_{E_R}(\mathbf{w})$ and $P_{E_I}(\mathbf{w})$ with respect to \mathbf{w} can be shown to be respectively

$$\begin{aligned} \nabla P_{E_R}(\mathbf{w}) &= \frac{\gamma}{2N_{sb} \sqrt{2\pi} \sigma_n \sqrt{\mathbf{w}^H \mathbf{w}}} \sum_{i=1}^{N_{sb}} e^{-\frac{(\bar{y}_{R_i}^{(l,q)} - c_{R_1}(u_l - 1))^2}{2\sigma_n^2 \mathbf{w}^H \mathbf{w}}} \\ &\times \left(\frac{\bar{y}_{R_i}^{(l,q)} - c_{R_1}(u_l - 1)}{\mathbf{w}^H \mathbf{w}} \mathbf{w} - \bar{\mathbf{x}}_i^{(l,q)} + (u_l - 1)\mathbf{p}_1 \right), \quad (26) \end{aligned}$$

$$\begin{aligned} \nabla P_{E_I}(\mathbf{w}) &= \frac{\gamma}{2N_{sb} \sqrt{2\pi} \sigma_n \sqrt{\mathbf{w}^H \mathbf{w}}} \sum_{i=1}^{N_{sb}} e^{-\frac{(\bar{y}_{I_i}^{(l,q)} - c_{R_1}(u_q - 1))^2}{2\sigma_n^2 \mathbf{w}^H \mathbf{w}}} \\ &\times \left(\frac{\bar{y}_{I_i}^{(l,q)} - c_{R_1}(u_q - 1)}{\mathbf{w}^H \mathbf{w}} \mathbf{w} + j\bar{\mathbf{x}}_i^{(l,q)} + (u_q - 1)\mathbf{p}_1 \right), \quad (27) \end{aligned}$$

where $\bar{\mathbf{x}}_i^{(l,q)} \in \mathcal{X}_{l,q}$. With the gradient $\nabla P_{E_B}(\mathbf{w}) = \nabla P_{E_R}(\mathbf{w}) + \nabla P_{E_I}(\mathbf{w})$, the optimisation problem (25) can be solved iteratively using a gradient algorithm, such as the simplified conjugate gradient algorithm [17]. The rotating operation (8) should be applied after each iteration, to ensure a real and positive c_1 .

It is worth emphasising that there exist infinitely many global MSER solutions which forms an infinite half line in the beamforming weight space, just as in the minimum BER (MBER) beamforming for BPSK and QPSK systems [17],[20]. This fact actually helps in numerical optimisation, as any point in this line is a global MSER solution. In our experience, we have not come across a case in which the optimisation algorithm converges to some local minima of the

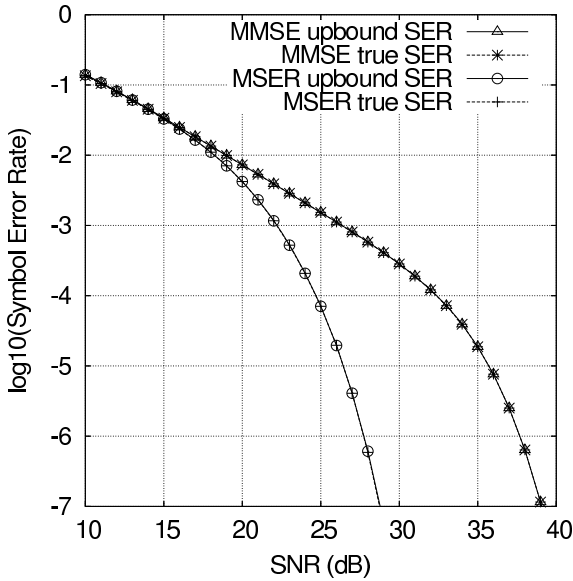


Fig. 2. True SER and its upper bound comparison of the two beamforming designs for the 16-QAM stationary-channel system employing three-element antenna array to support four users with $\text{SIR}_i = 0$ dB, $2 \leq i \leq 4$.

SER surface. Of course, if we normalise the weight vector to a unit length, then there exists only a single global MSER solution, just as in the BPSK case [28],[29].

In our previous study for the MBER beamforming [17],[20] we have demonstrated that the MBER solution offers greater user capacity and is significantly more robust to the near-far effects, in comparison with the MMSE benchmark. These desired properties are equally valid in the present MSER solution. Here we demonstrate that the true SER (16) and its upper bound (24) are practically indistinguishable. The beamforming system used is a 16-QAM stationary-channel system employing three-element antenna array to support four users, and all the interfering users and the desired user have an equal power. The true SER $P_E(\mathbf{w})$ and its upper bound $P_{E_B}(\mathbf{w})$ are plotted in Fig. 2 for both the MMSE and MSER solutions, where it can be seen that $P_E(\mathbf{w})$ and $P_{E_B}(\mathbf{w})$ are indistinguishable. This is unsurprising since the term $P_{E_R}(\mathbf{w})P_{E_I}(\mathbf{w})$ is negligible in comparison with the dominant part $P_{E_R}(\mathbf{w}) + P_{E_I}(\mathbf{w})$.

IV. ADAPTIVE MSER BEAMFORMING

In practice, the system matrix \mathbf{P} is unknown (except its first column). Therefore adaptive implementation is required to realise the MSER beamforming. To adaptively implement the MMSE solution, the unknown second-order statistics can be estimated based on a block of training data. Furthermore, by considering a single-sample “estimate” of the MSE, the stochastic adaptive algorithm known as the LMS is derived. A similar adaptive implementation strategy can be adopted for adaptive MSER beamforming. The PDF $p(y)$ of $y(k)$ can be estimated using the Parzen window estimate [24]-[26] based on a block of training data. This leads to an estimated SER for the beamformer. Minimising this estimated SER based on a gradient optimisation yields an approximated MSER solution. To derive a sample-by-sample adaptive algorithm, consider a

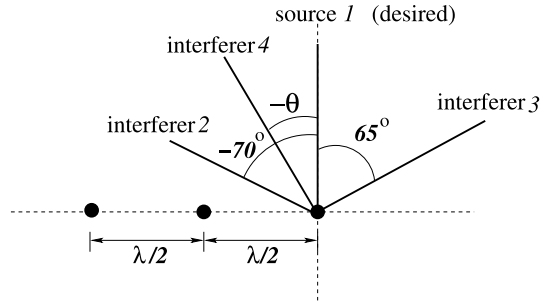


Fig. 3. Locations of the user sources with respect to the three-element linear array with $\lambda/2$ element spacing, λ being the wavelength, where $\theta < 65^\circ$.

single-sample “estimate” of $p(y)$

$$\tilde{p}(y, k) = \frac{1}{2\pi\rho_n^2} e^{-\frac{|y-y(k)|^2}{2\rho_n^2}} \quad (28)$$

and the corresponding one-sample SER “estimate” $\tilde{P}_{E_B}(\mathbf{w}, k)$. Using the instantaneous stochastic gradient of $\nabla \tilde{P}_{E_B}(\mathbf{w}, k) = \nabla \tilde{P}_{E_R}(\mathbf{w}, k) + \nabla \tilde{P}_{E_I}(\mathbf{w}, k)$ with

$$\begin{aligned} \nabla \tilde{P}_{E_R}(\mathbf{w}, k) &= \frac{\gamma}{2\sqrt{2\pi}\rho_n} e^{-\frac{(y_{R_1}(k) - \hat{\epsilon}_{R_1}(k)(b_{R_1}(k) - 1))^2}{2\rho_n^2}} \\ &\quad \times (-\mathbf{x}(k) + (b_{R_1}(k) - 1)\hat{\mathbf{p}}_1) \end{aligned} \quad (29)$$

and

$$\begin{aligned} \nabla \tilde{P}_{E_I}(\mathbf{w}, k) &= \frac{\gamma}{2\sqrt{2\pi}\rho_n} e^{-\frac{(y_{I_1}(k) - \hat{\epsilon}_{I_1}(k)(b_{I_1}(k) - 1))^2}{2\rho_n^2}} \\ &\quad \times (j\mathbf{x}(k) + (b_{I_1}(k) - 1)\hat{\mathbf{p}}_1) \end{aligned} \quad (30)$$

gives rise to the stochastic gradient adaptive LSER algorithm

$$\mathbf{w}(k+1) = \mathbf{w}(k) + \mu \left(-\nabla \tilde{P}_{E_B}(\mathbf{w}(k), k) \right), \quad (31)$$

$$\hat{\mathbf{c}}_1(k+1) = \mathbf{w}^H(k+1)\hat{\mathbf{p}}_1, \quad (32)$$

$$\mathbf{w}(k+1) = \frac{\hat{\mathbf{c}}_1(k+1)}{|\hat{\mathbf{c}}_1(k+1)|} \mathbf{w}(k+1), \quad (33)$$

where $\hat{\mathbf{p}}_1$ is an estimated \mathbf{p}_1 , and (32) and (33) implement the weight rotation operation. The step size μ and the kernel width ρ_n are the two algorithmic parameters that should be set appropriately in order to ensure an adequate performance in terms of convergence rate and steady-state SER misadjustment.

Theoretical proof for convergence of this LSER algorithm is very difficult if not impossible and is beyond the scope of this correspondence. We point out that this LSER algorithm belongs to the general stochastic gradient-based adaptive algorithm investigated in [30]. Therefore, the results of local convergence analysis presented in [30] is applicable here. Our previous investigations [22] have suggested that the LSER algorithm behaves well, has a reasonable convergence speed, and is consistently outperforms the LMS algorithm in terms of the achievable SER. Influence of the two algorithmic parameters of the LSER algorithm, namely μ and ρ_n , to the SER performance will be investigated in the following simulation. As emphasised in Section II, the column of the system matrix associated with the desired user, namely \mathbf{p}_1 , must be known in receiver. Usually, the steering vector \mathbf{s}_1

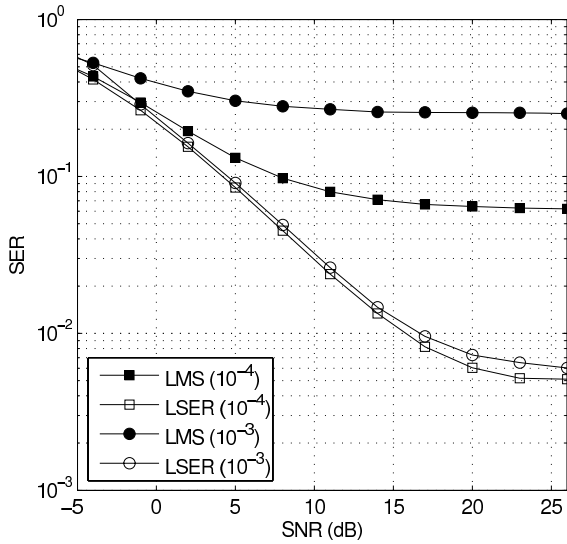


Fig. 4. Comparison of SER performance for the two normalised Doppler frequencies $\bar{f}_D = 10^{-4}$ and 10^{-3} with the minimum spatial separation $\theta = 27^\circ$. The LMS algorithm has a step size $\mu = 0.0002$, while the LSER algorithm has a step size $\mu = 0.00005$ and a kernel width $\rho_n = 4\sigma_n$.

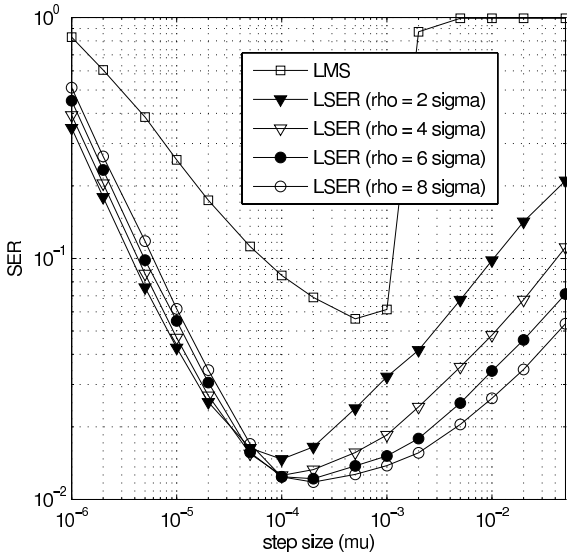


Fig. 5. Influence of the adaptive algorithm's parameters to the SER performance, given $\theta = 27^\circ$, $\bar{f}_D = 10^{-4}$ and average SNR = 15 dB.

associated with the desired user is known at receiver. The desired user's channel, A_1 , can always be estimated accurately during training. Thus, in the following simulation study, we assume a perfect \mathbf{p}_1 at receiver.

V. SIMULATION STUDY

The system consisted of four sources and a three-element antenna array. Fig. 3 shows the locations of the desired source and the interfering sources graphically, where the angular separation between the desired user and the interfering user 4 was $\theta < 65^\circ$. Note that the performance of a beamforming receiver depends on the minimum angular separation between the desired user and the interfering users (in this case θ), and whether or not the desired user is at the broadside of the antenna array is not too critical. We first performed an extensive investigation for the stationary case, where the

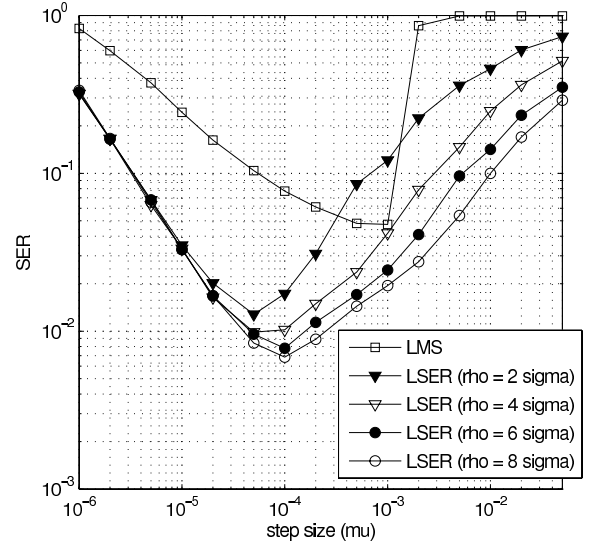


Fig. 6. Influence of the adaptive algorithm's parameters to the SER performance, given $\theta = 27^\circ$, $\bar{f}_D = 10^{-4}$ and average SNR = 30 dB.

simulated channel conditions A_i , $1 \leq i \leq 4$, were constant. Space limitation precludes the inclusion of these stationary results. Rather, we concentrated on presenting the fading simulation results.

The modulation scheme was 64-QAM. Fading channels were simulated, where magnitudes of A_i for $1 \leq i \leq 4$ were Rayleigh processes with the normalised Doppler frequency \bar{f}_D and each channel A_i had the root mean power of $\sqrt{0.5} + j\sqrt{0.5}$. Thus the average $\text{SIR}_i = 0$ dB for $2 \leq i \leq 4$. Continuously fluctuating fading was used, which provided a different fading magnitude and phase for each transmitted symbol. The transmission frame structure consisted of 50 training symbols followed by 450 data symbols. Decision-directed adaptation was employed during data transmission, in which the adaptive beamforming detector's decision $\hat{b}_1(k)$ was used to substitute for $b_1(k)$. The SER of an adaptive beamforming detector was calculated using the 450 data symbols of the frame based on Monte Carlo simulation averaging over at least 2×10^5 frames, depending on the value of \bar{f}_D . Two initialisations were used for the LSER algorithm, where the initial weight vector $\mathbf{w}(0)$ was initialised to either the MMSE solution (corresponding to the initial channel conditions) or $[0.1 + j0.0 \ 0.1 + j0.0 \ 0.1 + j0.0]^T$, and the performance were observed to be very similar for these two initialisations.

Given the minimum angular separation $\theta = 27^\circ$, Fig. 4 compares the SER of the adaptive LSER beamformer with that of the LMS-based one, for the two normalised Doppler frequencies $\bar{f}_D = 10^{-4}$ and 10^{-3} . It can be seen from Fig. 4 that the SER performance of the LSER beamformer degraded only slightly when the fading rate increased from $\bar{f}_D = 10^{-4}$ to 10^{-3} . This demonstrates that the LSER algorithm has an excellent tracking ability, capable of operating in fast fading conditions. We next investigated the influence of the adaptive algorithm's parameters. Given $\bar{f}_D = 10^{-4}$, Fig. 5 show the influence of the adaptive algorithm's parameters, μ for the LMS, and μ and ρ_n for the LSER, on the SER performance for a low average SNR value of 15 dB (Note this was 64-QAM system), while Fig. 6 depicts the results for a high

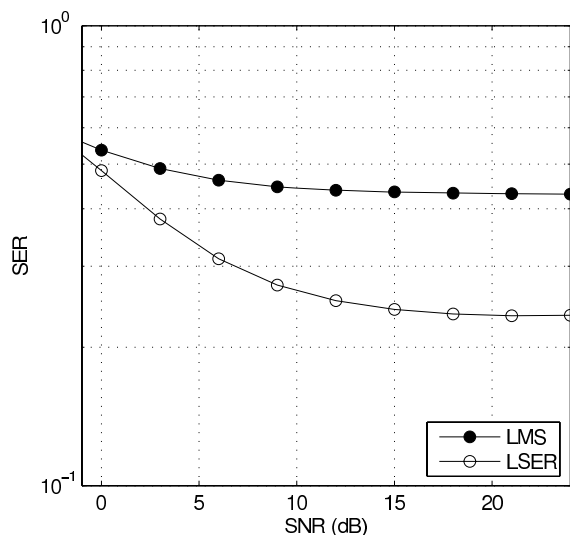


Fig. 7. Comparison of average SER performance for the normalised Doppler frequency $\bar{f}_D = 10^{-3}$ with the minimum spatial separation θ uniformly distributed in $[20^\circ, 50^\circ]$. The LMS algorithm has a step size $\mu = 0.0002$, while the LSER algorithm has a step size $\mu = 0.00005$ and a kernel width $\rho_n = 4\sigma_n$.

average SNR value of 30 dB. These results also explain how we came to use $\mu = 0.0002$ for the LMS and $\mu = 0.00005$ and $\rho_n = 4\sigma_n$ for the LSER in the simulation. Lastly, given $\bar{f}_D = 10^{-3}$, we varied the minimum angular separation θ uniformly in $[20^\circ, 50^\circ]$ and averaged the SER performance. The results are plotted in Fig. 7.

VI. CONCLUSIONS

An adaptive MSER beamforming technique has been proposed for multiple antenna aided multiuser communication systems with QAM signalling. It has been demonstrated that the MSER beamforming design can provide significant performance enhancement, in terms of the system SER, over the standard MMSE design. An adaptive implementation of the MSER beamforming solution has been realised using the stochastic gradient adaptive algorithm known as the LSER technique. The fading simulation results presented in this study clearly show that the adaptive LSER beamforming is capable of operating successfully in fast fading conditions and it consistently outperforms the adaptive LMS beamforming benchmark.

REFERENCES

- [1] J.H. Winters, J. Salz, and R. D. Gitlin, "The impact of antenna diversity on the capacity of wireless communication systems," *IEEE Trans. Commun.*, vol. 42, no. 2, pp. 1740–1751, 1994.
- [2] J. Litva and T. K. Y. Lo, *Digital Beamforming in Wireless Communications*. London: Artech House, 1996.
- [3] L. C. Godara, "Applications of antenna arrays to mobile communications, Part I: Performance improvement, feasibility, and system considerations," *Proc. IEEE*, vol. 85, no. 7, pp. 1031–1060, 1997.
- [4] R. Kohno, "Spatial and temporal communication theory using adaptive antenna array," *IEEE Personal Commun.*, vol. 5, no. 1, pp. 28–35, 1998.
- [5] J. H. Winters, "Smart antennas for wireless systems," *IEEE Personal Commun.*, vol. 5, no. 1, pp. 23–27, 1998.

- [6] P. Vandenameele, L. van Der Perre, and M. Engels, *Space Division Multiple Access for Wireless Local Area Networks*. Boston: Kluwer Academic Publishers, 2001.
- [7] J. S. Blogh and L. Hanzo, *Third Generation Systems and Intelligent Wireless Networking—Smart Antenna and Adaptive Modulation*. Chichester: John Wiley, 2002.
- [8] A. Paulraj, R. Nabar, and D. Gore, *Introduction to Space-Time Wireless Communications*. Cambridge: Cambridge University Press, 2003.
- [9] A. J. Paulraj, D. A. Gore, R. U. Nabar, and H. Bölcskei, "An overview of MIMO communications—a key to gigabit wireless," *Proc. IEEE*, vol. 92, no. 2, pp. 198–218, 2004.
- [10] D. Tse and P. Viswanath, *Fundamentals of Wireless Communication*. Cambridge, UK: Cambridge University Press, 2005.
- [11] B. Widrow and S. D. Stearns, *Adaptive Signal Processing*. Englewood Cliffs, NJ: Prentice-Hall, 1985.
- [12] S. Haykin, *Adaptive Filter Theory*, 3rd edition. Upper Saddle River, NJ: Prentice-Hall, 1996.
- [13] S. Chen, L. Hanzo, and N. N. Ahmad, "Adaptive minimum bit error rate beamforming assisted receiver for wireless communications," in *Proc. ICASSP 2003*, Hong Kong, China, Apr. 2003, vol. IV, pp. 640–643.
- [14] A. Wolfgang, N. N. Ahmad, S. Chen, and L. Hanzo, "Genetic algorithm assisted minimum bit error rate beamforming," in *Proc. VTC 2004-Spring*, May 2004, pp.142–146.
- [15] I. D. S. Garcia, J. J. S. Marciano, Jr., and R. D. Cajote, "Normalized adaptive minimum bit-error-rate beamformers," in *Proc. IEEE Region 10 TENCON Conf.*, Nov. 2004, vol.2, pp. 625–628.
- [16] Y.-H. Liu and Y.-H. Yang, "Adaptive minimum bit error rate multitarget array algorithm," in *Proc. IEEE 6th CAS Symp. Emerging Technologies: Frontiers of Mobile and Wireless Communication*, May 2004, vol. 2, pp. 745–748.
- [17] S. Chen, N. N. Ahmad, and L. Hanzo, "Adaptive minimum bit error rate beamforming," *IEEE Trans. Wireless Commun.*, vol. 4, no. 2, pp. 341–348, 2005.
- [18] L.-Y. Fan, H.-B. Zhang, and H. Chen, "Minimum bit error rate beamforming for pre-FFT OFDM adaptive antenna array," in *Proc. VTC 2005-Fall*, Sept. 2005, vol. 6, pp. 359–363.
- [19] S. Chen, L. Hanzo, N. N. Ahmad, and A. Wolfgang, "Adaptive minimum bit error rate beamforming assisted QPSK receiver," in *Proc. ICC 2004*, vol. 6, pp. 3389–3393.
- [20] S. Chen, L. Hanzo, N. N. Ahmad, and A. Wolfgang, "Adaptive minimum bit error rate beamforming assisted receiver for QPSK wireless communication," *Digital Signal Processing*, vol. 15, no. 6, pp. 545–567, 2005.
- [21] L. Hanzo, S. X. Ng, T. Keller, and W. Webb, *Quadrature Amplitude Modulation: From Basics to Adaptive Trellis-Coded, Turbo-Equalised and Space-Time Coded OFDM, CDMA and MC-CDMA Systems*. Chichester, UK: John Wiley and IEEE Press, 2004.
- [22] S. Chen, L. Hanzo, and B. Mulgrew, "Adaptive minimum symbol-error-rate decision feedback equalization for multi-level pulse-amplitude modulation," *IEEE Trans. Signal Processing*, vol. 52, no. 7, pp. 2092–2101, 2004.
- [23] C.-C. Yeh and J. R. Barry, "Adaptive minimum symbol-error rate equalization for quadrature-amplitude modulation," *IEEE Trans. Signal Processing*, vol. 51, no. 12, pp. 3263–3269, 2003.
- [24] E. Parzen, "On estimation of a probability density function and mode," *The Annals of Mathematical Statistics*, vol. 33, pp. 1066–1076, 1962.
- [25] B. W. Silverman, *Density Estimation*. London: Chapman Hall, 1996.
- [26] A. W. Bowman and A. Azzalini, *Applied Smoothing Techniques for Data Analysis*. Oxford: Oxford University Press, 1997.
- [27] J. M. Cioffi, G. P. Dudevoir, M. V. Eyuboglu, and G. D. Forney, Jr., "MMSE decision-feedback equalizers and coding—part I: equalization results," *IEEE Trans. Commun.*, vol. 43, no. 10, pp. 2582–2594, 1995.
- [28] X.-F. Wang, W.-S. Lu, and A. Antoniou, "Constrained minimum-BER multiuser detection," *IEEE Trans. Signal Processing*, vol. 48, no. 10, pp. 2903–2909, 2000.
- [29] S. Chen, A. K. Samangan, B. Mulgrew, and L. Hanzo, "Adaptive minimum-BER linear multiuser detection for DS-SS signals in multipath channels," *IEEE Trans. Signal Processing*, vol. 49, no. 6, pp. 1240–1247, 2001.
- [30] R. Sharma, W. A. Sethares, and J. A. Bucklew, "Asymptotic analysis of stochastic gradient-based adaptive filtering algorithms with general cost functions," *IEEE Trans. Signal Processing*, vol. 44, no. 9, pp. 2186–2194, 1996.